

Bifurcation of robust heteroclinic cycles in spherically invariant systems with $\ell = 3, 4$ mode interaction

Pascal Chossat¹ and Philippe Beltrame²

¹ laboratoire J-A Dieudonné (CNRS-UNSA) Parc Valrose, 06108 Nice Cedex 02, FRANCE,

² Dept. Physique, Université d'Avignon, 33 rue Pasteur - 84000 Avignon

E-mail: chossat@unice.fr

Abstract. Bifurcation with spherical symmetry and mode interaction is known to produce robust heteroclinic cycles between axisymmetric steady-states. The case of mode interaction with representations of $\mathbf{SO}(3)$ of degrees $\ell = 1$ and 2 has been studied in the context of the onset of convection in a spherical shell and central gravity force by [3] and [6] who explained certain numerical observations made in 1986 by Friedrich and Haken [11]. This problem has recently regained interest thanks to the launch of an experiment of convection between two concentric spheres in the International Space Station, thus providing a system with (nearly) spherical symmetry (GeoFlow project, see [9]). In this case however, the onset of convection cannot be excited by modes of degree ℓ smaller than 3 due to technical constraints. Motivated initially by this experiment, we have analyzed the occurrence of robust heteroclinic cycle in the case of $\ell = 3, 4$ mode interaction. This case is highly complex but, applying the methods of equivariant bifurcation theory, we have shown the existence of (generalized) robust heteroclinic cycles involving, not only axisymmetric states, but also and principally states with cubic symmetry. These objects are observable in the numerical simulations of the dynamics on the center manifold. We provide video clips showing the corresponding evolution of the pattern on the sphere.

AMS classification scheme numbers: 34C37, 37C80, 37G40, 37L20

1. Introduction

Evolution equations which are invariant under a linear action of the group $\mathbf{O}(3)$ are known to possess heteroclinic cycles, i.e invariant sets consisting of equilibria P_1, \dots, P_k such that the unstable manifold of P_j is included in the stable manifold of $P_{j+1} \pmod k$ in a structurally robust way (robust heteroclinic cycles are defined and discussed in [8]). The existence of these objects can be proved by bifurcation methods under certain conditions: 1) steady-state bifurcation occurs via mode interaction between irreducible representations of $\mathbf{O}(3)$ of degrees ℓ and $\ell + 1$; 2) the coefficients of the quadratic terms of the equation on the center manifold satisfy certain relations which we shall make

precise later. It turns out that these two conditions are generically fulfilled when the initial problem is the (classical) model of Rayleigh-Bénard convection in a spherical shell (see [2]). The case when $\ell = 1$, which is the simplest situation, has been analyzed in details and has been fully solved in [6]. It was shown that heteroclinic cycles in the above sense do indeed exist but are part of larger invariant sets which are called *generalized heteroclinic cycles* and which have been shown to be asymptotically stable. It was also shown that a robust heteroclinic cycle did still exist when the spherical shell was allowed to rotate (slowly) around an axis.

Recently some interest has grown about the case of convection of a fluid in a spherical shell with aspect ratio such that the onset of convection arises with mode interaction $\ell = 3$ and 4. This was in relation with the preparation of an experiment supported by the European Space Agency and named GeoFlow which consists of a spherical vessel filled with a fluid subjected to an electrophoretic central force [9]. This device is placed in the International Space Station in order to simulate a self-gravitating fluid. For technical reasons the aspect ratio of the spherical shell cannot be too small and the first unstable spherical modes are expected to be of degree $\ell = 3$ or 4. Numerical simulations near onset, using a center manifold approach in the case of mode interaction, have shown flow regimes which are quite suggestive of the presence of an attracting heteroclinic cycle involving steady states with cubic and/or tetrahedral isotropies [4]. Direct simulations show the same behaviour for some time but the flow always stabilizes on a steady-state with tetrahedral symmetry after a few switches [13]. We interpret this contradiction by the fact that the equations for the modes with $\ell = 4$ on the center manifold undergo a transcritical bifurcation of *unstable* steady-states (this is a well-known fact, see [7]), but have a quadratic term which is not very large and allows for a "bending back" of this branch with stable solutions above the turning point [12]. Then the equations for the modes with $\ell = 3$ generate the heteroclinic behaviour for the $\ell = 4$ steady-states. However it is likely that this "bending back" goes beyond the validity domain of the center manifold approximation, which would explain why the intermittent behaviour does not persist in the direct numerical model. In the Rayleigh-Bénard convection model, this quadratic term has a coefficient usually very close to 0 due to similar form of the gravity force and buoyancy force (see [2], [16]). This is a general fact valid for any even value of ℓ and it has allowed for a description of a large family of heteroclinic cycles in the $\ell, \ell + 1$ mode interaction for this problem [5]. However in the experimental device, the gravity field is replaced by an electrophoretic field which has a radial dependence in r^{-5} instead of r^{-2} for the buoyancy field, and this prevents the quadratic term in the $\ell = 4$ equations from being small (except possibly for special values of the Prandtl number). Moreover the heteroclinic cycles found in [5] are most probably always parts of more complex invariant sets and no stability assessment has been made except in the case $\ell = 1$ where it was precisely shown that the heteroclinic cycle is in fact embedded in a "generalized heteroclinic cycle" as was said above. To be complete it must also be said that in the classification of [5] (Theorem 5.5), the case $\ell = 3$ contains a mistake: indeed in this case precisely, a topological obstruction exists in the 2-dimensional space $\mathbf{D}_4 \oplus \mathbb{Z}_2^c$

(set of points which are fixed by the subgroup $\mathbf{D}_4 \oplus \mathbb{Z}_2^c$), preventing the existence of connections between axisymmetric states in this plane. This is one more reason to have a closer look at this case.

Our aim in this paper is to investigate the occurrence of generalized heteroclinic cycles in the $\ell = 3, 4$ mode interaction under conditions which are compatible with onset of Rayleigh-Bénard convection. When numerical simulations of the flow on the center manifold are performed, a great variety of complex spatiotemporal regimes can be observed near bifurcation, depending on coefficient and parameter values. We have focused on the simplest possible situations. We show that robust generalized heteroclinic cycles connecting axisymmetric steady-states with ones having cubic symmetry can bifurcate. In [5], such objects involving steady-states with cubic symmetry were found to exist only for high values of ℓ : 8, 9 and 13. Moreover these generalized heteroclinic cycles can be attracting.

We begin by a description of the geometry of the $\mathbf{O}(3)$ group action in the 3, 4 interaction and we describe the equivariant structure of the equations on the center manifold (coefficients listed in the appendix). Then we look at the primary and (some of the) secondary bifurcations of steady-states. In Section 3 we give a precise definition of the generalized heteroclinic cycles and we show the existence of such objects under certain conditions which are satisfied for an open set of parameter values.

2. Bifurcation with $\ell = 3, 4$ mode interaction with $\mathbf{O}(3)$ symmetry

2.1. Isotropy types, equations on the center manifold

A very basic step when studying a bifurcation problem with symmetry, is to determine the isotropy types of the group action on the center manifold and the corresponding fixed-point subspaces. Let us recall that given $x \in X$ vector space with a representation $g \rightarrow T(g)$ of a group G ($G = \mathbf{O}(3)$ in our case), we define the *isotropy subgroup* of x to be the subgroup $\{g \in G / T(g)x = x\}$. The *fixed-point subspace* associated with an isotropy subgroup H is the set $\{y \in X / T(H)y = y\}$. The fundamental property of G -equivariant evolution equations (or dynamical systems) is that given an initial condition $x_0 \in \text{Fix}(H)$, the trajectory $\{x(t)\}$ lies entirely in $\text{Fix}(H)$. It is clear that if $H \subset H'$ are two isotropy subgroups, then $\text{Fix}(H) \supset \text{Fix}(H')$. Also, two subspaces $\text{Fix}(H)$ and $\text{Fix}(H')$ are symmetric to each other, i.e. there exists an element $g \in G$ such that $\text{Fix}(H') = T(g)\text{Fix}(H)$, if and only if H and H' are conjugated by an element in G (namely by g). The conjugacy class of an isotropy subgroup is called an *isotropy type*. From the above comments, it is clear that isotropy types are partially ordered.

Natural irreducible representations of $\mathbf{O}(3)$ of degree ℓ are spanned by the spherical harmonics $Y_\ell^m(\vartheta, \varphi)$ ($-\ell \leq m \leq +\ell$). Therefore the dimension of the center manifold in the 3, 4 mode interaction is 16. Moreover, we know that the antipodal symmetry S acts trivially when ℓ is even and as $-Id$ when ℓ is odd. We denote by \mathbb{Z}_2^c the 2-element group of S . This is the notation which was introduced by Golubitsky, Stewart and Schaeffer

in [14] and which we will follow more generally to name the isotropy subgroups (see a correspondence table with Schoenflies notation in [8]).

The diagram in Figure 1 below shows the tree of isotropy types for the $\ell = 3, 4$ mode interaction with $\mathbf{O}(3)$ symmetry. This diagram has been obtained from the informations contained in [7] where notations of the groups are also explained. The numbers in parenthesis on the left side indicate the dimensions of the fixed-point subspaces on each corresponding line. More on the structure of these subspaces will be given in next sections.

The isotropy types with one dimensional fixed point subspaces are the "pure" $\ell = 4$ mode isotropies $\mathbf{O}(2) \oplus \mathbb{Z}_2^c$ (axisymmetric modes) and $\mathbb{O} \oplus \mathbb{Z}_2^c$ (cubic symmetry modes). We know from the Equivariant Branching Lemma [14] that corresponding branches of equilibria bifurcate from the trivial state. In the "generic" case, it is known that the branches are transcritical (presence of quadratic terms in the bifurcation equations) and unstable [7]. We shall be interested in the case when the pure quadratic terms have a vanishing or nearly vanishing coefficient, a situation which occurs in classical Rayleigh-Bénard convection. In this case, not only these bifurcated branches can bend back and gain stability, but also other types of solutions with lower isotropy can bifurcate through secondary and tertiary bifurcations. The unfolding of this quadratic degeneracy has been studied in details in [12]. The complete picture looks already quite complicated in the pure $\ell = 4$ case. The coupling with $\ell = 3$ modes makes the problem even more complicated, as can be already seen from the diagram of isotropy types. We shall therefore focus on some specific, relatively simple situations where the existence of heteroclinic orbits can be proved and where the number of steady-states involved in the construction of heteroclinic cycles is limited.

Let $X = (x_{-3}, \dots, x_3)$ denote the component along the $\ell = 3$ spherical harmonics Y_3^j , and $Y = (y_{-4}, \dots, y_4)$ denote the component along the $\ell = 4$ spherical harmonics Y_4^k . Note that, $Y_\ell^{-m} = (-1)^m \bar{Y}_\ell^m$ and therefore the same holds for the coordinates (real space). We list in the table below the components of the fixed-point subspaces with dimension lower than 6. These isotropy types are the important ones for the subsequent study. The reader can easily complete the list by looking at the tables in [7]. Our convention is that coordinates which are not indicated should be set equal to 0. Also, we write (general notation): $z = z_r + iz_i \in \mathbb{C}$.

Let us now write the equations on the center manifold. Only the leading terms need be considered here. The context of this paper is the onset of convection in a self-gravitating spherical shell with uniformly heated inner boundary. This assumption, as shown in [5] (in [2] in a more general context), has strong consequences on the signs of coefficients of the leading part of the equations on the center manifold. Because S acts non trivially when $\ell = 3$ but trivially when $\ell = 4$, the "pure" mode, 9-dimensional subspace associated with $\ell = 4$ is flow-invariant (this is $Fix(\mathbb{Z}_2^c)$). We perform a generic change of variables in the parameters if necessary, so that there are two free parameters μ_1 and μ_2 such that the $\ell = 3$ modes become unstable when $\mu_1 > 0$ and the $\ell = 4$ modes become unstable when $\mu_2 > 0$.

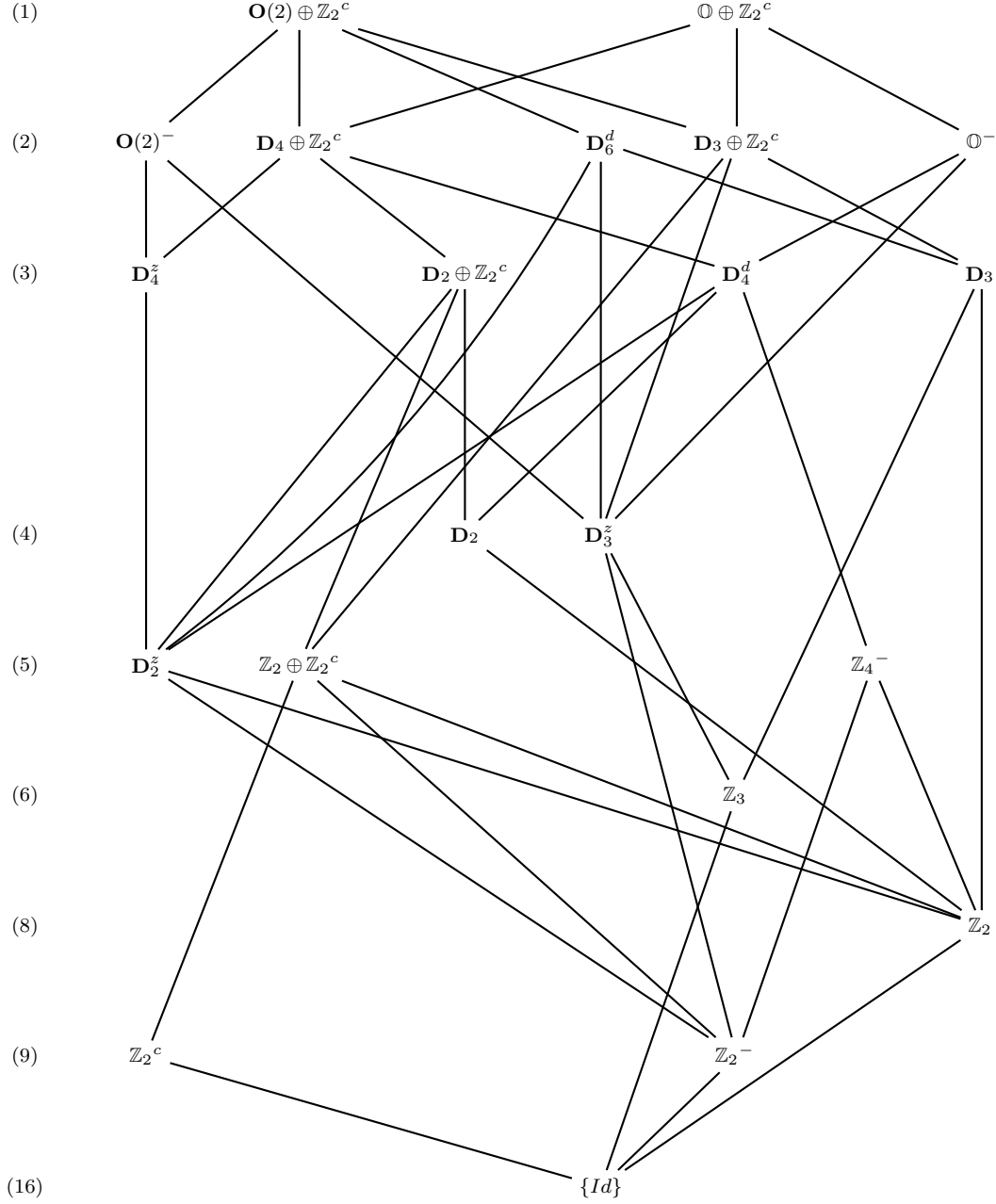


Figure 1. The isotropy types for the $\ell = 3, 4$ mode interaction. Numbers on the left indicate dimension of corresponding fixed point subspaces

Then the leading part of the equations in these coordinates read

$$\dot{x}_j = \mu_1 x_j + \beta Q_j^{(1)}(x_{-3}, \dots, x_3, y_{-4}, \dots, y_4) + \gamma_1 \|X\|^2 x_j + \gamma_2 C_j^{(1)}(x_{-3}, \dots, x_3) \quad (1)$$

$$\dot{y}_k = \mu_2 y_k + b Q_k^{(2)}(x_{-3}, \dots, x_3) + c Q_k^{(3)}(y_{-4}, \dots, y_4) + d_1 \|Y\|^2 y_k + d_2 C_k^{(2)}(y_{-4}, \dots, y_4) \quad (2)$$

where the Q 's denote quadratic terms and the C 's denote cubic terms which are given explicitly in the annex. In the context of Rayleigh-Bénard convection in a spherical

| Isotropy H | $Fix(H)$ | Isotropy H | $Fix(H)$ |
|---------------------------------------|-------------------------------|--------------------------------------|---|
| $\mathbf{O}(2) \oplus \mathbb{Z}_2^c$ | y_0 | $\mathbf{D}_2 \oplus \mathbb{Z}_2^c$ | (y_0, y_{2r}, y_{4r}) |
| $\mathbb{O} \oplus \mathbb{Z}_2^c$ | $y_{4r} = \pm \eta y_0$ | \mathbf{D}_4^d | (x_{2i}, y_0, y_{4r}) |
| $\mathbf{O}(2)^-$ | (x_0, y_0) | \mathbf{D}_3 | (x_{3i}, y_0, y_{3r}) |
| $\mathbf{D}_4 \oplus \mathbb{Z}_2^c$ | (y_0, y_{4r}) | \mathbf{D}_2 | $(x_{2i}, y_0, y_{2r}, y_{4r})$ |
| \mathbf{D}_6^d | (x_{3r}, y_0) | \mathbf{D}_3^z | $(x_0, x_{3r}, y_0, y_{3r})$ |
| $\mathbf{D}_3 \oplus \mathbb{Z}_2^c$ | (y_0, y_{3r}) | \mathbf{D}_2^z | $(x_0, x_{2r}, y_0, y_{2r}, y_{4r})$ |
| \mathbb{O}^- | $(x_{2i}, y_{4r} = \eta y_0)$ | $\mathbb{Z}_2 \oplus \mathbb{Z}_2^c$ | $(y_0, y_2, \bar{y}_2, y_4, \bar{y}_4)$ |
| \mathbf{D}_4^z | (x_0, y_0, y_{4r}) | \mathbb{Z}_4^- | $(x_2, \bar{x}_2, y_0, y_4, \bar{y}_4)$ |

Table 1. Fixed-point subspaces for representatives of the isotropy types such that $\dim Fix(H) \leq 5$. We have noted $\eta = \sqrt{\frac{5}{14}}$. Another useful representation of $Fix(\mathbb{O} \oplus \mathbb{Z}_2^c)$ is $y_{3r} = \nu y_0$ with $\nu = \sqrt{\frac{10}{7}}$.

shell, the coefficients satisfy certain relations which, using the normalization applied to compute the equivariant polynomials listed in the Appendix, are as follows [5]:

Hypotheses (H1):

- (i) $b \sim -2\beta$. We do not lose generality by assuming that $\beta = -1$ (after a suitable change of time scale).
- (ii) $\gamma_1 + 20\gamma_2 < 0$,
- (iii) $d_1 + d_2 < 0$, $j = 1, \dots, 4$,
- (iv) $c \sim 0$ will be considered as an additional parameter. In all the following we restrict to the case $c \geq 0$.

2.2. Primary branches of steady-states

There are two primary bifurcated branches of steady-states which correspond to the maximal isotropy types (those with $\dim Fix(H) = 1$). We detail these solutions and compute the eigenvalues of the Jacobian of the vector field at these solutions, in order to study later their stable and unstable manifolds.

2.2.1. The axisymmetric equilibria On the axis $Fix(\mathbf{O}(2) \oplus \mathbb{Z}_2^c)$ the (scalar) bifurcation equation reads

$$0 = \mu_2 y_0 + 9cy_0^2 + (d_1 + d_2)y_0^3.$$

It follows that the bifurcated equilibria satisfy the relation

$$\mu_2 = -9cy_0 - (d_1 + d_2)y_0^2 \tag{3}$$

A turning point exists at $y_0 = -\frac{9c}{2(d_1+d_2)}$ and by H-(iii) the parabola is oriented towards $y_0 > 0$ in the (μ_2, y_0) plane. Even in the limit $c = 0$, the two branches of the parabola correspond to symmetrically distinct states.

We denote by α_{\pm} these branches of axisymmetric equilibria along the Y_4^0 component. They generate two-dimensional $\mathbf{O}(3)$ orbits of equilibria. In order to determine their stable and unstable manifolds we need to compute the eigenvalues of the Jacobian matrix $L_{\alpha_{\pm}}$ of the vector field linearized at α_{\pm} , hence to determine first the isotypic decomposition of the action of $\mathbf{O}(2) \oplus \mathbb{Z}_2^c$ in the 3, 4 representation of $\mathbf{O}(3)$. A straightforward (and classical) analysis shows that $L_{\alpha_{\pm}}$ decomposes into two 1×1 and seven 2×2 diagonal blocks along the coordinates $x_0, y_0, (x_j, \bar{x}_j)$ ($j = 1, 2, 3$) and (y_m, \bar{y}_m) ($m = 1, 2, 3, 4$) respectively. The block in the (y_1, \bar{y}_1) subspace is the 0 matrix, corresponding to the fact that this plane is tangent to the $\mathbf{O}(3)$ orbit of α_{\pm} [7]. The other eigenvalues are listed in the following table 2 where y_0 is the coordinate of α_{\pm} .

| Eigenvalues | Multiplicity | Eigenspaces |
|--|--------------|----------------------|
| $\sigma_0^{\alpha} = \mu_1 - 6y_0$ | 1 | x_0 |
| $\sigma_1^{\alpha} = \mu_1 - y_0$ | 2 | $\{x_1, \bar{x}_1\}$ |
| $\sigma_2^{\alpha} = \mu_1 + 7y_0$ | 2 | $\{x_2, \bar{x}_2\}$ |
| $\sigma_3^{\alpha} = \mu_1 - 3y_0$ | 2 | $\{x_3, \bar{x}_3\}$ |
| $\lambda_0^{\alpha} = 9cy_0 + (2d_1 + d_2)y_0^2$ | 1 | y_0 |
| $\lambda_1^{\alpha} = 0$ | 2 | $\{y_1, \bar{y}_1\}$ |
| $\lambda_2^{\alpha} = -20cy_0 + 5/2d_2y_0^2$ | 2 | $\{y_2, \bar{y}_2\}$ |
| $\lambda_3^{\alpha} = -30cy_0 - 45/28d_2y_0^2$ | 2 | $\{y_3, \bar{y}_3\}$ |
| $\lambda_4^{\alpha} = 5cy_0 - 20/7d_2y_0^2$ | 2 | $\{y_4, \bar{y}_4\}$ |

Table 2. Eigenvalues of the linearized vector field at $\alpha = \alpha_{\pm}$

2.2.2. The cubic equilibria Let us consider the axis $Fix(\mathbb{O} \oplus \mathbb{Z}_2^c)$ defined by the relation $y_{4r} = \sqrt{5/14}y_0$. The bifurcation equation along this axis parametrized by y_0 reads

$$0 = \mu_2 y_0 + 14cy_0^2 + \left(\frac{12}{7}d_1 - \frac{16}{49}d_2\right)y_0^3$$

and therefore that bifurcated branches are given by

$$\mu_2 = -14cy_0 - \left(\frac{12}{7}d_1 - \frac{16}{49}d_2\right)y_0^2 \quad (4)$$

We shall assume:

Hypothesis (H2): $3d_1 - \frac{4}{7}d_2 < 0$.

(H2) combined with (H1-iii) is equivalent to $d_1 < 0$ and $21/4d_1 < d_2 < -d_1$. Then the parabola is oriented towards $y_0 > 0$ in the (μ_2, y_0) plane. Even in the limit $c = 0$ the two branches of the parabola correspond to symmetrically distinct states.

We note these solutions $\beta = \beta_+$ or β_- . They generate three-dimensional $\mathbf{O}(3)$ orbits of equilibria. The eigenvalues of the Jacobian matrix $L_{\beta_{\pm}}$ of the vector field linearized at β_{\pm} are listed in the following table 3, together with the corresponding eigenspaces. Here again the multiplicity and eigenspaces follow from the isotypic decomposition of the action of $\mathbb{O} \oplus \mathbb{Z}_2^c$ in the $\ell = 3, 4$ representation of $\mathbf{O}(3)$. The convention is that coordinates which do not appear in the definition of eigenspaces must be set equal to 0. The β_{\pm} solutions are parametrized by their coordinate y_0 .

| Eigenvalues | Multiplicity | Eigenspaces |
|--|--------------|--|
| $\sigma_0^\beta = \mu_1 + 12y_0$ | 1 | $\{x_{2i}\}$ |
| $\sigma_1^\beta = \mu_1 - 6y_0$ | 3 | $\{x_0, x_3 = -\frac{\sqrt{15}}{3}\bar{x}_1\}$ |
| $\sigma_2^\beta = \mu_1 + 2y_0$ | 3 | $\{x_{2r}, x_3 = \frac{\sqrt{15}}{5}\bar{x}_1\}$ |
| $\lambda_0^\beta = 14cy_0 + (24/7d_1 - 32/49d_2)y_0^2$ | 1 | $\{y_{4r} = \sqrt{\frac{5}{14}}y_0\}$ |
| $\lambda_1^\beta = 0$ | 3 | $\{y_{4i}, y_3 = -\frac{\sqrt{7}}{7}\bar{y}_1\}$ |
| $\lambda_2^\beta = -10cy_0 + 40/7d_2y_0^2$ | 2 | $\{y_{2r}, y_{4r} = -\sqrt{\frac{7}{10}}y_0\}$ |
| $\lambda_3^\beta = -40cy_0 + 10/7d_2y_0^2$ | 3 | $\{y_{2i}, y_3 = \sqrt{7}\bar{y}_1\}$ |

Table 3. Eigenvalues of the linearized vector field at $\beta = \beta_\pm$

2.3. Submaximal bifurcations

There are two kinds of branches of steady-states with non maximal isotropy in this problem: 1) secondary branching in the pure $\ell = 4$ mode subspace, due to the quadratic degeneracy $c \simeq 0$; 2) branching occurring in mixed mode subspaces (with μ_1 as a natural bifurcation parameter). The first case, which is independent of the mode interaction, has been studied in detail by [12]. Equilibria with $\mathbf{D}_k \oplus \mathbb{Z}_2^c$, $k = 2, 3, 4$, have been shown to bifurcate in certain regions of parameter space. This combined with the bifurcations in the $\ell = 3$ directions makes a very complicated bifurcation diagram which we do not intend to describe here. Our aim here is rather to focus on the simple case of *submaximal* bifurcation, *i.e.* branching of solutions with submaximal isotropy [8], [7]. In our case, this means branching in one of the invariant planes listed in Table 1.

2.3.1. Bifurcations in the pure $\ell = 4$ invariant planes According to Fig. 1 there are two kinds of such planes. Let us choose the representatives given in Table 1, *i.e.* with coordinates resp. $Fix(\mathbf{D}_4 \oplus \mathbb{Z}_2^c) = \{y_0, y_{4r}\}$ and $Fix(\mathbf{D}_3 \oplus \mathbb{Z}_2^c) = \{y_0, y_{3r}\}$. Each of them contains the axis $Fix(\mathbf{O}(2) \oplus \mathbb{Z}_2^c) = \{y_0\}$ and two copies of the axes of cubic isotropy $\mathbb{O} \oplus \mathbb{Z}_2^c$: $\{y_{4r} = \pm\eta y_0\}$ in $Fix(\mathbf{D}_4 \oplus \mathbb{Z}_2^c)$ and $\{y_{3r} = \pm\nu y_0\}$ in $Fix(\mathbf{D}_3 \oplus \mathbb{Z}_2^c)$ (where $\eta = \sqrt{\frac{5}{14}}$, $\nu = \sqrt{\frac{10}{7}}$).

It is a known fact that, when the quadratic coefficient c is fixed non zero, the bifurcated branches with maximal isotropy (types α and β) are transcritical and no other solutions occur [7]. However we assume the degeneracy hypothesis (H1-iv). Let us focus first on the plane $P = \{y_0, y_{4r}\}$. Writing $u = y_0$ and $v = y_{4r}$ to simplify notations, the equations read

$$\dot{u} = \mu_2 u + c(9u^2 + 14v^2) + d_1 u(u^2 + 2v^2) + d_2 u(u^2 - \frac{26}{7}v^2) \quad (5)$$

$$\dot{v} = \mu_2 v + 14cuv + d_1 v(u^2 + 2v^2) + d_2 v(-\frac{13}{7}u^2 + \frac{30}{7}v^2) \quad (6)$$

We note β_\pm (resp. $\tilde{\beta}_\pm$) the equilibria on the invariant axis $\{y_{4r} = \eta y_0\}$ (resp. $\{y_{4r} = -\eta y_0\}$). Equilibria off the invariant axes (hence with $\mathbf{D}_4 \oplus \mathbb{Z}_2^c$ isotropy) must

satisfy the conditions

$$u = \frac{7c}{4d_2} \text{ and} \quad (7)$$

$$\mu_2 = -\frac{7c^2}{16d_2^2} (7d_1 + 43d_2) - (2d_1 + \frac{30}{7}d_2)v^2 \quad (8)$$

We see that the bifurcation from α (axisymmetric) equilibria in the plane P is a *pitchfork* and occurs at the μ_2 value

$$\mu_2^\alpha = -(7d_1 + 43d_2) \frac{7c^2}{16d_2^2}.$$

When $c > 0$ and $d_2 < 0$ the branching occurs off the α_- equilibrium. Let us denote by $\gamma, \tilde{\gamma}$ these equilibria. As μ_2 is increased, they move closer to the invariant axes with cubic isotropy until they cross them at the value

$$\mu_2^\beta = -(21d_1 + 94d_2) \frac{c^2}{4d_2^2}.$$

This corresponds to a *transcritical* bifurcation from β and $\tilde{\beta}$ solutions. When $c > 0$ and $d_2 < 0$, the secondary bifurcations occur from the α_- branch (at μ_2^α) and from the branches β_- and $\tilde{\beta}_-$ (at μ_2^β). The latter correspond to the vanishing of the eigenvalue $\lambda_2^{\beta-}$ (see Table 3).

The phase diagram in the plane P when $0 < \mu_2 < \mu_2^\alpha$ looks like Fig. 2.

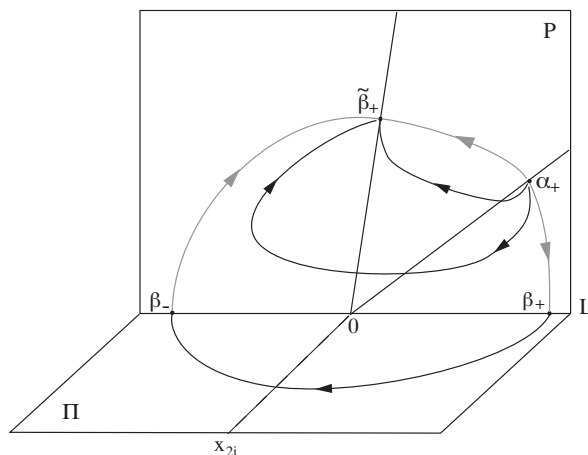


Figure 2. Phase portrait in $P = \text{Fix}(\mathbf{D}_4 \oplus \mathbb{Z}_2^c)$ when $0 < \mu_2 < \mu_2^\alpha$. Equilibria β_\pm and $\tilde{\beta}_\pm$ are exchanged by rotation $\phi = \pi/4$.

An examination of the eigenvalues in Tables 2 and 3 show that as long as $\mu < \mu_2^\beta$, there are no other secondary bifurcations in the pure $\ell = 4$ modes. It can be shown that indeed no other branch of equilibria exist in this case [12]. This means in particular that the secondary bifurcations with $\mathbf{D}_3 \oplus \mathbb{Z}_2^c$ isotropy, which can be described in a very similar manner in the plane (y_0, y_{3r}) , occur at values of μ_2 larger than μ_2^β .

More precisely, let us now consider the dynamics in $Fix(\mathbf{D}_3 \oplus \mathbb{Z}_2^c)$. We use the notation $y_0 = u, y_{3r} = w$. Then,

$$\dot{u} = \mu_2 u + c(9u^2 - 21w^2) + d_1 u(u^2 + 2w^2) + d_2 u(u^2 - \frac{17}{14}w^2) \quad (9)$$

$$\dot{w} = \mu_2 w - 21cuw + d_1 w(u^2 + 2w^2) + d_2 w(-\frac{17}{28}u^2 - \frac{5}{56}w^2) \quad (10)$$

The invariant axes with cubic isotropy are defined by $w = \pm\sqrt{\frac{10}{7}}u$ and the branches of equilibria on these axes is given by

$$\mu_2 = 21cu - (\frac{27}{7}d_1 - \frac{36}{49}d_2)u^2 = 21cu - \frac{9}{4}(\frac{12}{7}d_1 - \frac{16}{49}d_2)u^2 \quad (11)$$

The bifurcation scenario is similar to the one in the plane P , except for the following. Comparing the above expression with (4), we deduce that the solutions with $u > 0$ (resp. $u < 0$) belong to the orbit of β_- (resp. β_+). Moreover, the secondary bifurcations occur when the eigenvalues λ_3^α or λ_3^β vanish, and this happens at values of μ_2 which are larger than μ_2^β . In particular, when μ is smaller than

$$\hat{\mu}_2^\alpha = -8(168d_1 + 17d_2)\frac{c^2}{d_2^2}$$

there are no secondary equilibria and the phase diagram looks like in Figure 3.

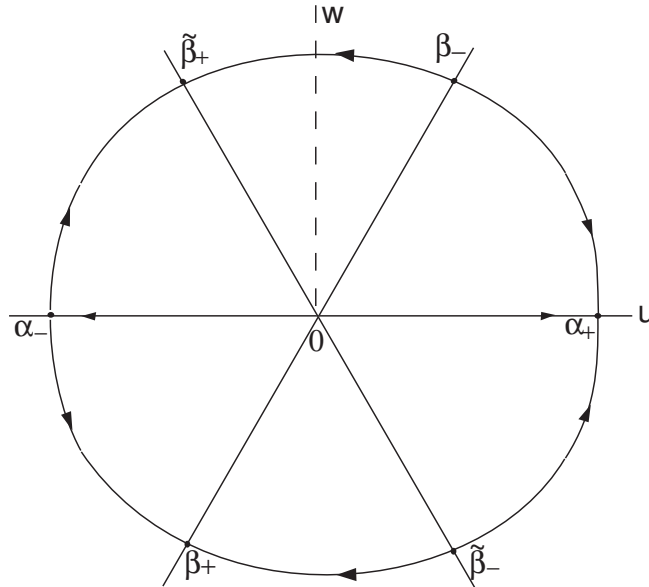


Figure 3. Phase portrait in $Fix(\mathbf{D}_3 \oplus \mathbb{Z}_2^c)$ when $\mu_2 < \hat{\mu}_2^\alpha$. Notations β_\pm mean that the equilibria belong to the group orbits of β_\pm .

2.3.2. Invariant "mixed-mode" planes According to the isotropy tree in Fig. 1 there are three such planes: $Fix(\mathbf{O}(2)^-)$, $Fix(\mathbf{D}_6^d)$ and $Fix(\mathbf{O}^-)$. The first two planes contain the invariant axis $Fix(\mathbf{O}(2) \oplus \mathbb{Z}_2^c)$ while the third plane contains the axis $Fix(\mathbf{O} \oplus \mathbb{Z}_2^c)$.

Using the expressions given in the Appendix for the quadratic equivariants, it is easy to check that the conditions of application of Proposition 1 of [2] are met when (H1) is satisfied. Therefore heteroclinic orbits connecting the two bifurcated equilibria lying on the invariant axis exist for an open set of parameter values.

Let us be more specific about the plane $\Pi = \text{Fix}(\mathbb{O}^-)$, which can be defined by the coordinates x_{2i} and $y_{4r} = \eta y_0$ ($\eta = \sqrt{5/14}$). The axis of symmetry $\{y_{4r} = \eta y_0\}$ contains the equilibria β_{\pm} . Using y_0 as a parameter for this axis, the equations for the flow on Π read

$$\dot{x}_{2i} = \mu_1 x_{2i} + 12x_{2i}y_0 + (2\gamma_1 + 20\gamma_2)x_{2i}^3 \quad (12)$$

$$\dot{y}_0 = \mu_2 y_0 + 14cy_0^2 - 14x_{2i}^2 + (12/7d_1 - 16/49d_2)y_0^3 \quad (13)$$

The bifurcation scenario for this kind of planar system is classical and we don't go into details of the calculations (see [3]). Let us assume first that $c = 0$ and fix $\mu_2 > 0$ in order to insure existence of branches with maximal isotropy (thanks to H1 and H2). We set $12/7d_1 - 16/49d_2 = D$ and

$$\tilde{\mu}_1 = -12\sqrt{\frac{\mu_2}{-D}}$$

($D < 0$ by hypothesis H2). Then as μ_1 is varied the following events occur:

- For $\mu_1 < \tilde{\mu}_1$, there exist no equilibria off the invariant axis and β_{\pm} are both sinks in Π .
- At $\mu_1 = \tilde{\mu}_1$ a pitchfork bifurcation occurs from β_+ off the axis. We note δ and $\tilde{\delta}$ the bifurcated equilibria with isotropy \mathbb{O}^- (which are exchanged by taking the coordinate x_{2i} to its opposite).
- As μ_1 is increased further, a Hopf bifurcation occurs from δ (and $\tilde{\delta}$).
- The two limit cycles grow until they collide with the stable manifold of the origin. Then they disappear and two *saddle-sink connections* from β_+ to β_- are established at a value $\mu_1 = \hat{\mu}_1$ which satisfies $\tilde{\mu}_1 < \hat{\mu}_1 < 0$.
- The equilibria $\delta, \tilde{\delta}$ die off at the origin in a "reverse" bifurcation when $\mu_1 = 0$.
- The heteroclinic orbit from β_+ to β_- persists until a new pitchfork bifurcation occurs from β_- at a positive value of μ_1 .

These properties persist when c is taken non zero but small.

Similar scenarios occur in $\text{Fix}(\mathbf{O}(2)^-)$ and in $\text{Fix}(\mathbf{D}_6^d)$, with secondary bifurcation from the axisymmetric states α_{\pm} . It can be easily checked that heteroclinic orbits between these states can coexist in both planes, however the eigenvalues at α_- , resp. α_+ along these connections, which are given by λ_0^α and λ_3^α , have the same sign, and therefore these orbits cannot form heteroclinic cycles. In the next section we shall consider situations where such connections do not exist.

3. Robust generalized heteroclinic cycles

As it was already shown in [6], the usual definition of a heteroclinic cycle (as given in [8]) is not sufficient to describe recurrent heteroclinic behaviour in systems with

$\mathbf{O}(3)$ symmetry. Indeed it may happen that instead of a cycle, the set of heteroclinic orbits makes a non trivial (closed) network with multidimensional connections between equilibria. Hereafter we give a suitable definition of a *robust generalized heteroclinic cycle* in order to take account of this generality. Given an equilibrium ξ of (1)-(2), we denote by $O\xi$ its $\mathbf{O}(3)$ orbit and more generally, given a submanifold M in phase space, we set $OM = \{g \cdot M \mid g \in \mathbf{O}(3)\}$ where $g \cdot$ denotes the action of $g \in \mathbf{O}(3)$. We also denote by W_ξ^s (resp. W_ξ^u) its stable (resp. unstable) manifold (see [8]). Note that, $OW_\xi^{s,u} = W_{O\xi}^{s,u}$. The following definition is stated for $\mathbf{O}(3)$ equivariant systems but is obviously generalized to any other group of symmetry.

Definition 1 *A set of $\mathbf{O}(3)$ orbits of saddle equilibria $O\xi_1, \dots, O\xi_n$, defines a generalized, $\mathbf{O}(3)$ invariant heteroclinic cycle (a GHC) if for any $j \in \{1, \dots, n\}$,*

$$W_{O\xi_j}^u \subset \bigcup_{k \neq j} W_{O\xi_k}^s.$$

The GHC itself is the union $\bigcup_j W_{O\xi_j}^u$. This definition is stronger than others because we request that all unstable trajectories be heteroclinic orbits in the GHC. On the other hand the manifolds of connections can be multidimensional and can follow multiple circuits.

We look for heteroclinic cycles which are *robust* under small $\mathbf{O}(3)$ -equivariant perturbations (equivariant structural stability). This can indeed happen if the following is true.

Condition for structural stability: whenever two equilibria ξ and ξ' in the GHC are connected, i.e. satisfy $W_\xi^u \cap W_{\xi'}^s \neq \emptyset$, then there exists an isotropy subgroup H such that the following properties hold (transversality conditions):

- (i) $\xi, \xi' \in \text{Fix}(H)$
- (ii) either ξ is a source or ξ' is a sink in $\text{Fix}(H)$,
- (iii) $W_\xi^u \cap W_{\xi'}^s \cap \text{Fix}(H) \neq \emptyset$

Our aim in this section is at finding such objects. We begin with the case when only α and β equilibria are involved. We look first at heteroclinic connections in $\text{Fix}(\mathbb{Z}_2^c)$ (pure $\ell = 4$ modes), then at connections involving both $\ell = 3$ and 4 modes (so-called "mixed modes"). Remark that our study does not exhaust all possible types of generalized heteroclinic cycles. In fact it is easy to find other types which can be deduced from those analyzed here and which however do not add better understanding of the problem.

3.1. Generalized heteroclinic cycles with α and β equilibria

3.1.1. Connections in $\text{Fix}(\mathbb{Z}_2^c)$

Proposition 1 *Suppose hypotheses (H1) and (H2) are satisfied and in addition $0 < \mu_2 < \mu_2^\alpha$. Then O_{β_+} (the $\mathbf{O}(3)$ orbit of equilibria β_+) is attracting in $\text{Fix}(\mathbb{Z}_2^c)$ and moreover the equilibria α_\pm and β_\pm satisfy the properties (i)-(iii) above.*

Proof. We rely on [12] to assert that under the conditions of the proposition, there are no secondary branches of equilibria. Moreover, the system is determined at cubic order, and this truncated vector field is a gradient (see [7]). Therefore there are no other non trivial bounded sets than α and β equilibria and heteroclinic orbits connecting them in $Fix(\mathbb{Z}_2^c)$ (note however that this gradient property prevents heteroclinic orbits to form a cycle.) Now, examination of the eigenvalues λ_j^α and λ_k^β (tables 2 and 3) show that under the conditions (H1) and (H2), β_+ is stable as a relative equilibrium (i.e. its $\mathbf{O}(3)$ orbit is stable) and there are no other stable equilibria. The second part of the proposition follows from the fact that the dynamics is bounded in $Fix(\mathbb{Z}_2^c)$ when conditions (H1)-(H2) are satisfied. This in turn follows from the fact that the quadratic form $d_1\|Y\|^4 + d_2Y \cdot C^{(2)}(Y)$ is negative, where $C^{(2)}(Y)$ is the cubic map defined in Table A5. The proof is straightforward if one assumes $|d_2|$ small. In fact, thanks to the assumption that c is close enough to 0, we can apply a theorem by M. Field [10] which states the existence of a *flow-invariant and attracting topological sphere* in $Fix(\mathbb{Z}_2^c)$. ■

Let us now be more precise on the phase portrait. Restricting to the planes $Fix(\mathbf{D}_4 \oplus \mathbb{Z}_2^c)$ and $Fix(\mathbf{D}_3 \oplus \mathbb{Z}_2^c)$, the pictures are like in Figures 2 and 3. It is more delicate to describe the phase portrait in higher dimensional fixed-point subspaces but it is instructive to consider the 3 dimensional $Fix(\mathbf{D}_2 \oplus \mathbb{Z}_2^c)$. This space contains three copies P, P' and P'' of $Fix(\mathbf{D}_4 \oplus \mathbb{Z}_2^c)$ which intersect all three on the same axis $L = Fix(\mathbb{O} \oplus \mathbb{Z}_2^c)$. Using coordinates (y_0, y_{2r}, y_{4r}) (see Table 1), these planes have equations $y_{2r} = 0$ and $y_{2r} = \pm(\frac{\sqrt{10}}{4}y_0 - \frac{\sqrt{7}}{2}y_{4r})$ and $L = \{y_{2r} = 0, y_{4r} = \sqrt{5/14}y_0\}$. The three planes are exchanged by the action of $N(\mathbf{D}_2)/\mathbf{D}_2 \simeq D_3$ (we note $N(\mathbf{D}_2)$ the normalizer of \mathbf{D}_2 in $\mathbf{SO}(3)$, which is known to be \mathbb{O} , see [14]). This structure is sketched in Fig. 4 below. Assuming the existence of the flow-invariant sphere, the bounded dynamics restricts to that sphere and can therefore be easily seen on a 2D picture (see Fig. 5). We see that β_+ and $\tilde{\beta}_+$ are sinks, β_- and β''_- have robust connections to α_- (in $Fix(\mathbf{D}_4 \oplus \mathbb{Z}_2^c)$) which itself has a robust connection to $\tilde{\beta}_+$. This combined with the phase portrait in $Fix(\mathbf{D}_3 \oplus \mathbb{Z}_2^c)$ (Fig. 3) gives a good description of the various connections in $Fix(\mathbb{Z}_2^c)$.

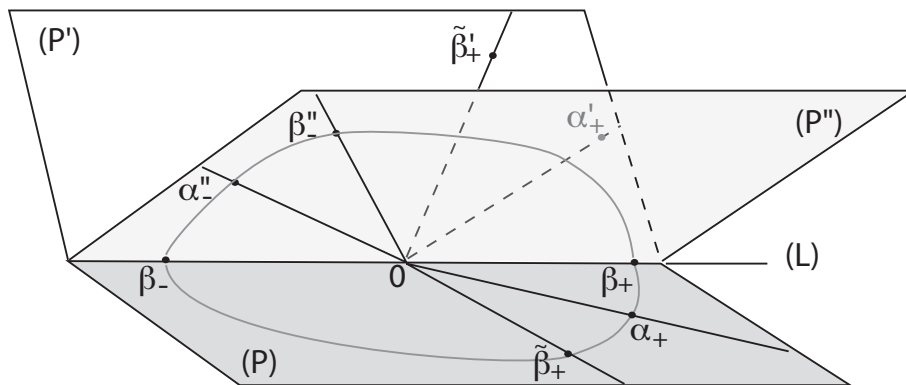


Figure 4. The subspace $Fix(\mathbf{D}_2 \oplus \mathbb{Z}_2^c)$.

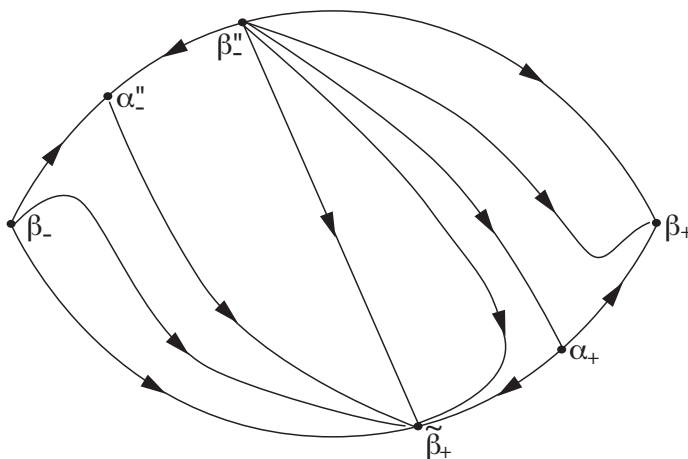


Figure 5. $Fix(\mathbf{D}_2 \oplus \mathbb{Z}_2^c)$: the phase portrait on the portion of invariant sphere bounded by P and P'' with $y_0 > 0$.

3.1.2. Connections involving $\ell = 3$ modes Since β_+ is a sink in $Fix(\mathbb{Z}_2^c)$, we look for its unstable manifold involving necessarily $\ell = 3$ perturbations and such that the conditions (i)-(iii) are met. We already know from Section 2.3.2 that saddle-sink connections between β_+ and β_- exist in the plane $\Pi = Fix(\mathbb{O}^-)$ when $\mu_1 > \hat{\mu}_1$ where $\hat{\mu}_1 < 0$. However there are constraints in order to insure that conditions (i)-(iii) above are satisfied. If $\mu_1 > 0$, the eigenvalues $\sigma_j^{\alpha^-}$ with $j = 1, 3$ are positive as well as $\sigma_1^{\beta^-}$, and then the problem becomes too complicated (although simple attractors like relative equilibria or relative periodic orbits can be numerically observed at certain parameter values). We therefore suppose $\mu_1 < 0$. Then clearly, from the expressions in Tables 2 and 3, the following is true: $\sigma_j^{\alpha^+} < 0$ ($j = 0, 1, 3$), $\sigma_2^{\alpha^-} < 0$, $\sigma_0^{\beta^-} < 0$, $\sigma_1^{\beta^+} < 0$ and $\sigma_2^{\beta^-} < 0$.

The following lemma shows that an open interval exists in which all the other eigenvalues are negative except $\sigma_0^{\beta^+} > 0$ which is a necessary condition for the saddle-sink connection in Π . Let y_{\pm}^{α} and y_{\pm}^{β} denote the values of y_0 at the equilibria α_{\pm} , resp. β_{\pm} , in Tables 2 and 3.

Lemma 1 *Assume (H1)-(H2) and $\mu_1 < 0$. Define $\mu_1' = -7y_+^{\alpha}$, $\mu_1'' = -2y_+^{\beta}$ (negative values). The following estimates hold:*

- (i) *if $\mu_1 < \min(\mu_1', \mu_1'')$, then $\sigma_j^{\alpha^-} < 0$ ($j = 0, 1, 3$), $\sigma_2^{\alpha^+} < 0$, $\sigma_1^{\beta^-} < 0$ and $\sigma_2^{\beta^+} < 0$;*
- (ii) *if $\mu_1 > 6\mu_1''$, then $\sigma_0^{\beta^+} > 0$.*
- (iii) *There exists a value $\tilde{d}_2 < 0$ such that the following is true: if $21/4d_1 < d_2 < \tilde{d}_2$, then $\mu_1'' < \mu_1'$ while if $0 > d_2 > \tilde{d}_2$, then $6\mu_1'' < \mu_1' < \mu_1''$.*

Proof. By Tables 2 and 3, the signs of eigenvalues in point (i) are satisfied if

$$\mu_1 < 6y_-^{\alpha}, \mu_1 < -7y_+^{\alpha}, \mu_1 < 6y_-^{\beta}, \mu_1 < -2y_+^{\beta}$$

and point (ii) is satisfied if

$$\mu_1 > -12y_+^{\beta}.$$

The point (ii) is therefore immediate. Solving (4) and (3) for y_0 , we find that

$$y_{\pm}^{\alpha} = \frac{1}{2(d_1 + d_2)} \left(-9c \mp \sqrt{81c^2 - 4(d_1 + d_2)\mu_2} \right) \quad (14)$$

$$y_{\pm}^{\beta} = \frac{1}{D} \left(-7c \mp \sqrt{49c^2 - D\mu_2} \right) \quad (15)$$

where $D = 12/7d_1 - 16/49d_2$. Recall that by our hypotheses, $D < 0$ and $d_1 + d_2 < 0$. Replacing these formulas in the above inequalities and using our hypotheses, point (i) follows without difficulty. To prove point (iii) one can also easily check the following: if $d_2 = 0$ then $6\mu_1'' < \mu_1' < \mu_1''$ while when $d_2 \rightarrow 21/4d_1$ (from above), then μ_1' is bounded and $\mu_1'' \rightarrow -\infty$. \blacksquare

The value $6\mu_1''$ corresponds to $\tilde{\mu}_1$ in Section 2.3.2. The determination of the lowest value $\hat{\mu}_1$ at which the saddle-sink connection $\beta_+ \rightarrow \beta_-$ is established, is very cumbersome. However in all the tests which have been done, it is observed numerically that $\hat{\mu}_1 < \mu_1''$. This leads us to making the following ansatz:

Ansatz 1 *In the hypotheses of Lemma 1, $\hat{\mu}_1 < \mu_1''$.*

It follows from lemma 1 that when d_2 is close enough to 0, $\mu_1' < \mu_1''$, therefore when μ_1 lies between these two values the eigenvalue $\sigma_2^{\alpha+}$ is positive while the saddle-sink connections $\beta_+ \rightarrow \beta_-$ exist in Π and all the other eigenvalues in the $\ell = 3$ directions remain negative. It turns out that $\sigma_2^{\alpha+}$ corresponds to the eigendirection transverse to the plane $P = \text{Fix}(\mathbf{D}_4 \oplus \mathbb{Z}_2^c)$ in the subspace $\text{Fix}(\mathbf{D}_4^d) = P \oplus \Pi$ (see Table 1). Therefore the unstable manifold of α_+ in $\text{Fix}(\mathbf{D}_4^d)$ is two-dimensional, with eigendirections y_{4r} (eigenvalue $\lambda_4^{\alpha+}$) in P and x_{2i} (eigenvalue $\sigma_2^{\alpha+}$) transversally to P . This situation is very similar to the one observed in the $\ell = 1, 2$ mode interaction [6]. It can be shown with the same proof that the flow in the space $\text{Fix}(\mathbf{D}_4^d)$, for d_2 and c in a neighborhood of 0, looks like in Fig. 6. In fact, as in the Proposition 4.6 of [6], one can even show the following

Proposition 2 *In addition to hypotheses (H1) and (H2) suppose that d_2 is close enough to 0 and the Ansatz 1 is true. Then there exists an open interval of (negative) values of μ_1 such that the full (4-dimensional) unstable manifold of α_+ is included in the stable manifold of the group orbit of β_+ in the 5-dimensional space $\text{Fix}(\mathbb{Z}_4^-)$.*

Proof. We exploit the fact that if $d_2 = 0$, then the problem in $\text{Fix}(\mathbb{Z}_4^-)$ is *identical* to the problem restricted to $\text{Fix}(\mathbb{Z}_2^-)$ in the $\ell = 1, 2$ interaction case which was studied in [6]. Indeed the geometry is similar, in particular we note that $N(\mathbb{Z}_4^-)/\mathbb{Z}_4^- \simeq \mathbf{O}(2)$ acts in the same manner in $\text{Fix}(\mathbb{Z}_4^-)$ than $N(\mathbb{Z}_2^-)/\mathbb{Z}_2^-$ does in the $\ell = 1, 2$ case. Moreover there is only one pure $\ell = 2$ cubic equivariant $\|Y\|^2 Y$, and if $d_2 = 0$ the same is true in the $\ell = 4$ case. The equations in $\text{Fix}(\mathbb{Z}_4^-)$ then read (at leading order):

$$\dot{x}_2 = \mu_1 x_2 + 7x_2 y_0 - \sqrt{70} \bar{x}_2 y_4 + (2\gamma_1 + 20\gamma_2) x_2^2 \bar{x}_2 \quad (16)$$

$$\dot{y}_0 = \mu_2 y_0 + c(9y_0^2 + 14y_4^2) - 14x_2 \bar{x}_2 + d_1 y_0 (y_0^2 + 2y_4 \bar{y}_4) \quad (17)$$

$$\dot{y}_4 = \mu_2 y_4 + 14c y_0 y_4 + \frac{\sqrt{70}}{2} x_2^2 + d_1 y_4 (y_0^2 + 2y_4 \bar{y}_4) \quad (18)$$

The proofs of Propositions 4.6 and 4.7 in [6] apply to this system, and taking d_2 close enough to 0 does not modify the result. Numerical computations show evidence that the result persists for a larger range of values of d_2 as well as of c . \blacksquare

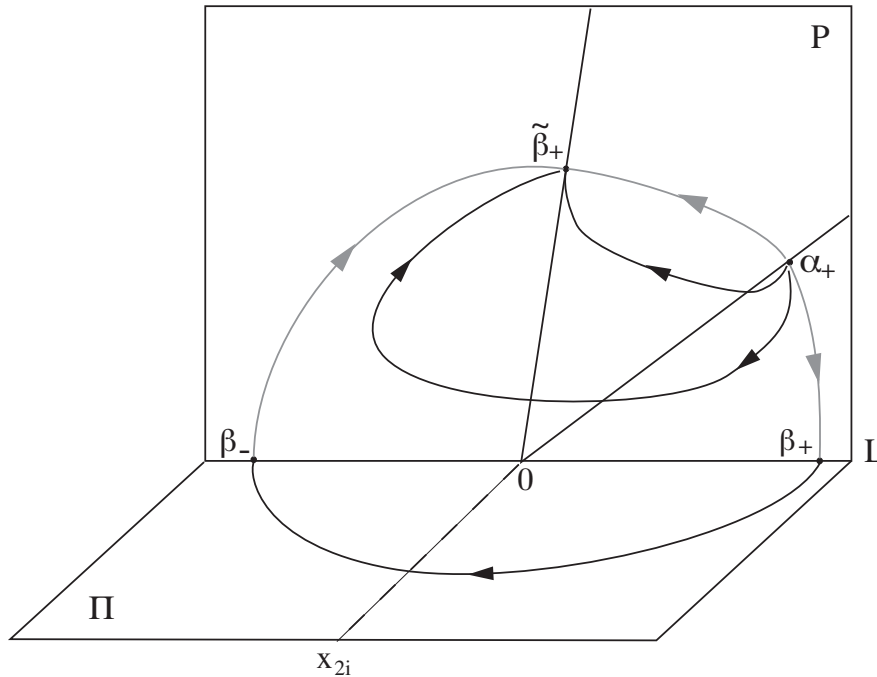


Figure 6. The phase portrait in $Fix(\mathbf{D}_4^d)$ (in grey the heteroclinic connections in P).

3.1.3. The generalized heteroclinic cycles We can summarize the previous results in the following theorem:

Theorem 1 *Assume hypotheses H1 and H2 and the ansatz 1 are true. Then, for open intervals of parameter values $\mu_1 < 0$ and $\mu_2 > 0$, a generalized heteroclinic cycle exists, which connects the $\mathbf{O}(3)$ -orbits of equilibria of α and β types and whose structure depends on the values of the coefficient d_2 :*

(i) *There exists a neighborhood I of 0 in \mathbb{R} such that when $d_2 \in I$, all four types α_{\pm} and β_{\pm} are involved in a structure which is described in Propositions 1 and 2 and sketched in Figure 7.*

(ii) *There exists a value \tilde{d}_2 , $21/4d_1 < \tilde{d}_2 < 0$, such that when $21/4d_1 < d_2 < \tilde{d}_2$, the generalized heteroclinic cycle has a simpler structure than in (i), involving α_+ and β_{\pm} only, according to the diagram of Figure 8.*

Proof of the Theorem. Point (i) is a direct consequence of Propositions 1 and 2. To prove point (ii) note first that equilibria γ and $\tilde{\gamma}$ with isotropy $\mathbf{D}_4 \oplus \mathbb{Z}_2^c$ bifurcate transcritically (and unstably) from β_- when $\mu_2 > \mu_2^{\beta}$, as shown in Section 2.3.1. Then the phase portrait Figure 5 (in $Fix(\mathbf{D}_2 \oplus \mathbb{Z}_2^c)$) is replaced by Figure 9 below. The

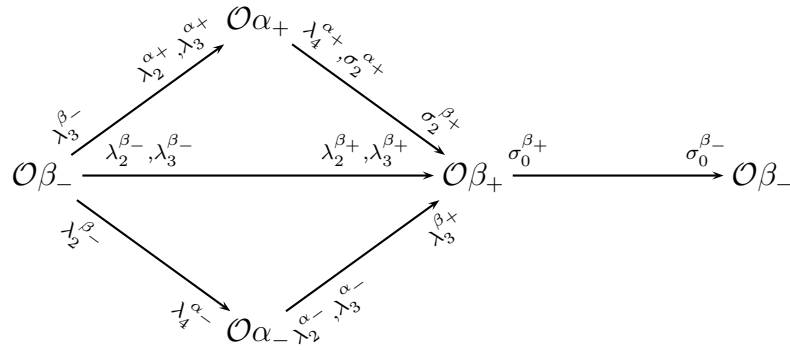


Figure 7. Scheme of the heteroclinic cycle when d_2 close to 0, showing the eigenvalues corresponding to the (manifolds of) connecting orbits

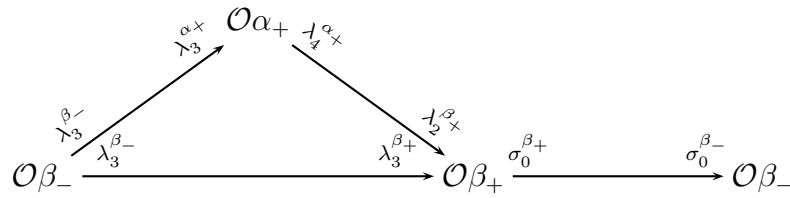


Figure 8. Scheme of the heteroclinic cycle when $d_2 < \tilde{d}_2$ and $\mu_2 > \mu_2^\beta$, showing the eigenvalues corresponding to the (manifolds of) connecting orbits.

heteroclinic cycle does not involve α_- anymore. Moreover if d_2 is large enough (in absolute value), an interval of values of μ_1 exists such that all eigenvalues involving $\ell = 3$ eigendirections are negative but $\sigma_0^{\beta+}$ which is positive due to the existence of the heteroclinic orbits in Π . In this case the heteroclinic cycle has a much simpler structure.

■

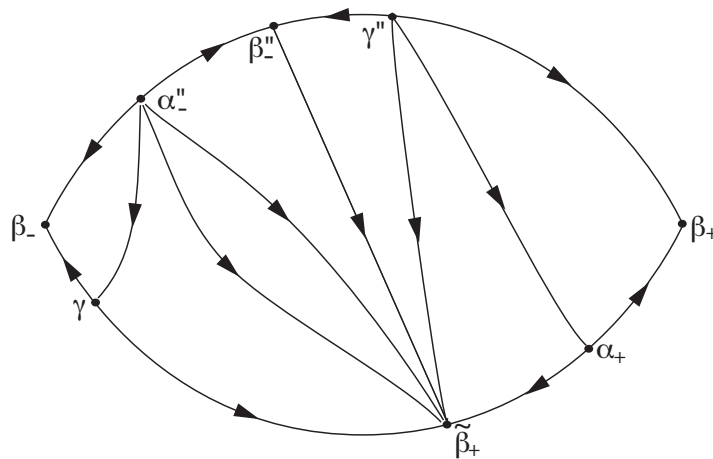


Figure 9. $Fix(\mathbf{D}_2 \oplus \mathbb{Z}_2^c)$: the phase portrait on the portion of invariant sphere bounded by P and P'' (see Fig. 5) in the case $\mu_2 > \mu_2^\beta$.

3.2. A simple heteroclinic cycle involving mixed-mode equilibria

We have seen in Section 2.3.2 that when $\mu_1 < \hat{\mu}_1 < 0$, the presence of a stable fixed point δ (and its symmetric $\tilde{\delta}$) in the plane Π prevented the existence of the saddle-sink connections in that plane. However if we now look at the 3-dimensional subspace $Fix(\mathbf{D}_4^d) = P \oplus \Pi$, a saddle-sink connection can exist in that subspace between δ (in Π) and $\tilde{\beta}_+$ (in P). The process by which such a connection is created is the following: first, a steady-state bifurcation from δ occurs off the plane Π at a value $\mu'_1 > \tilde{\mu}_1$. This new steady-state with \mathbf{D}_4^d symmetry is a sink. As μ_1 increases, it travels toward the plane P until it disappears in $\tilde{\beta}_+$. Then the saddle-sink connection is established. A completely similar situation holds in the $\ell = 1, 2$ interaction and was analyzed in more details in [3]. We refer to this paper for the formal proof of existence of this connection in the limits $c = 0, d_2 = 0$.

Once the saddle-sink heteroclinic connection exists, a heteroclinic cycle is set since $\tilde{\beta}_+$ belongs to the group orbit $\mathcal{O}\beta_+$ (see the diagram 19 below). Moreover this cycle is simple: it involves unstable manifold of dimension 1 only (in $Fix(\mathbb{O}^-)$). This was called a "type II" heteroclinic cycle by [3].

$$\mathcal{O}\beta_+ \longrightarrow \mathcal{O}\delta \longrightarrow \mathcal{O}\beta_+ \tag{19}$$

Variants of this cycle involving periodic orbits in Π do also exist for suitable parameter values.

3.3. Stability and numerical simulation of the heteroclinic cycles

The asymptotic stability of a "simple" heteroclinic cycle depends on the relative strength of the stable and unstable eigenvalues of the Jacobian matrix calculated at the equilibria which compose the cycle. Of particular relevance are the eigenvalues with eigendirections along the heteroclinic connections. General stability conditions for such cycles were derived by [15]. These conditions apply to the simple cycle (19), but not to the generalized heteroclinic cycles of Section 3.1.3. Indeed one of the conditions is that for each equilibrium in the cycle, its unstable manifold consist of points with the *same* isotropy type. This is clearly not the case for the cycles in Figures 7 and 8: for example the unstable manifold of β_- in the case of figure 8 intersects the strata of isotropy type $\mathbf{D}_3 \oplus \mathbb{Z}_2^c$ (connections to equilibria of type α_+), $\mathbf{D}_2 \oplus \mathbb{Z}_2^c$ and \mathbb{Z}_2^c (connections to equilibria of type β_+).

A similar situation holds in the $\ell = 1, 2$ mode interaction case, as shown in [6], however there the geometry was simpler and stability conditions could be derived by construction of a first return map using local orbit space reduction.

Here we are facing two kinds of difficulties. First, the generalized cycles are in fact *networks* of connections between equilibria, in which different itineraries are possible due to the multidimensionality of the connecting sets. Hence the question of which itinerary is indeed followed by the asymptotic dynamics arises. This problem was investigated

by [1] in a simpler context and no general answer exists so far. Secondly, the unstable manifold associated with the same eigenvalue $\lambda_3^{\beta-}$ (of multiplicity 3) is foliated with heteroclinic connections to α_+ equilibria as well as to β_+ equilibria, as indicated on the diagrams of Figures 7 and 8. Therefore it is likely that nonlinearities play a role in the asymptotic dynamics near these heteroclinic cycles.

The issue of finding the asymptotic stability conditions and minimal attracting sets for generalized heteroclinic cycles is therefore a difficult one and it goes beyond the aim of this paper, which is to present a new (and relevant) type of heteroclinic cycles occurring in systems with spherical symmetry. This issue will be the topic for a future work. Below we simply show on some examples the numerical evidence for asymptotic stability behaviour of the three types of generalized heteroclinic cycles which we have described in the previous section. These simulations have been realized on a Matlab code for the integration of the cubic order system. Videos showing the time evolution of the pattern associated with these time series can be seen on <http://www.math.unice.fr/~chossat>.

3.3.1. Asymptotic dynamics near the heteroclinic cycle of Figure 7 This cycle is numerically observed for a non empty set of values of the coefficients and parameters in the equations. Recall that it is assumed that d_2 (as well as c) is small in absolute value. In the following calculations we have taken:

$$\beta = 0.08, \quad b = -0.09, \quad c = 0.01, \quad \gamma_1 = -0.5, \quad \gamma_2 = -0.5/36, \quad d_1 = -1, \quad d_2 = -0.008.$$

The bifurcation parameter values are $\mu_1 = -0.09$ and $\mu_2 = 0.03$. Then a typical time series is shown in Fig. 10. This figure shows the time series (after transients have been eliminated) for the energy of the modes with $\ell = 3$ (in blue) and 4 (in red). It can be

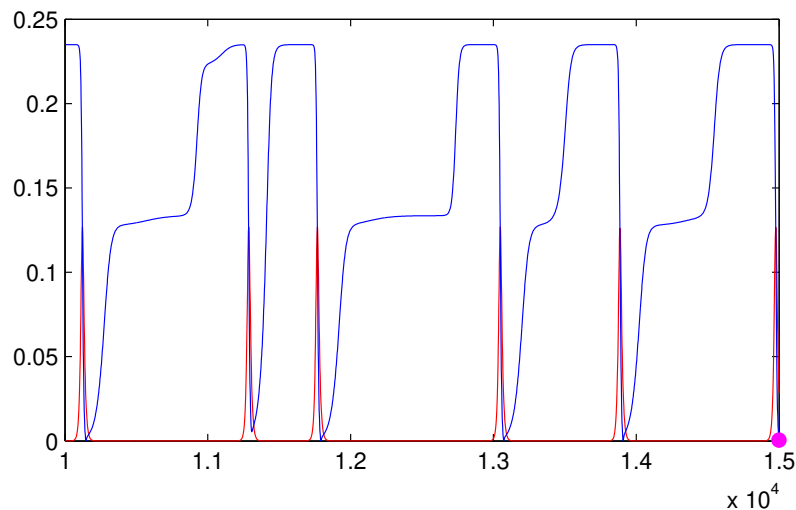


Figure 10. Time series of energies associated with the modes $\ell = 3$ (in blue) and 4 (in red) in the case of Figure 7.

observed on the video that the dynamics passes near the axisymmetric states of type

α_- , but never close to those of type α_+ . When $|d_2|$ is larger the flow between β_- and β_+ follows the connection in $\mathbf{D}_3 \oplus \mathbb{Z}_2^c$ and does not come close to axisymmetric states anymore.

3.3.2. Asymptotic dynamics near the heteroclinic cycle of Figure 8 We take the same coefficient values as in the previous subsection, except that now $d_2 = -1.6$. In this case the secondary steady-states γ exist and the cycle of Figure 8 is realized. The bifurcation parameter values are $\mu_1 = -0.1$ and $\mu_2 = 0.03$. Then a typical time series is shown in Fig. 11. On the corresponding video the axisymmetric steady-states are clearly not

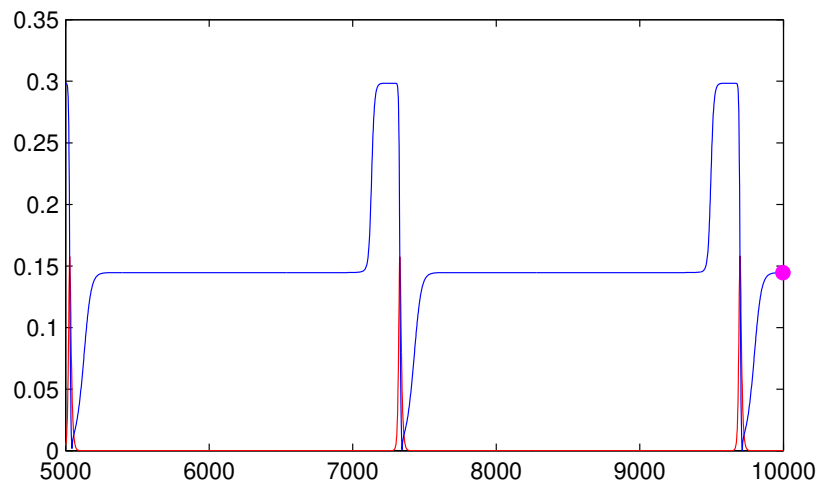


Figure 11. Time series of energies associated with the modes $\ell = 3$ (in blue) and 4 (in red) in the case of Figure 8.

present.

3.3.3. Asymptotic dynamics near the simple heteroclinic cycle of diagram (19) We take again $d_2 = 0.08$, all other coefficients identical to the previous ones, but now $\mu_1 = -0.13$. In this case the $\beta_+ \rightarrow \beta_-$ connections in $Fix(\mathbb{O}^-)$ are broken by mixed-mode steady-states which undergo saddle-sink connections in $Fix(D_4^d)$ to the $\tilde{\beta}_+$ equilibria. A typical time series is shown in Fig. 12.

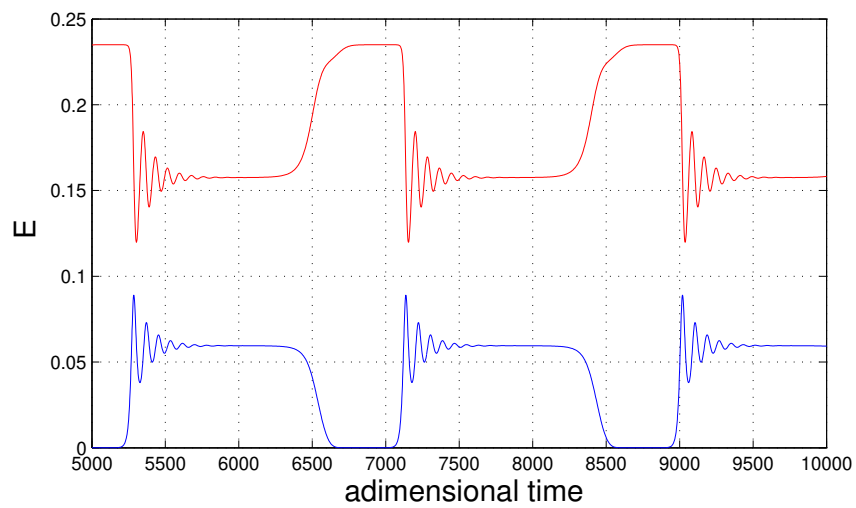


Figure 12. Time series of energies associated with the modes $\ell = 3$ (in blue) and 4 (in red) in the case of diagram (19).

Appendix A. The quadratic and cubic equivariant maps

In the tables below we list the coefficients of quadratic and cubic maps in equations (1) and (2). Conventions are as follows: Number m in the "Equation" column indicates the index of the component along the spherical harmonic Y_ℓ^m , with $\ell = 3$ or 4 depending on the map under consideration. We list only the coefficients for the components with $m = 0, \dots, +\ell$, since the components for negative m are obtained from the ones with positive m according to the rule $Y_\ell^{-m} = (-1)^m \overline{Y_\ell^m}$. The numbers in parenthesis in the column "terms" indicate the indices of the corresponding terms with the following convention: (i, j) for the quadratic terms $x_i y_j$ ($-3 \leq i \leq 3, -4 \leq j \leq 4$), (ij) for the terms $x_i x_j$ ($-3 \leq i \leq j \leq 3$) or $y_i y_j$ ($-4 \leq i \leq j \leq 4$), and (ijk) for the cubic terms $y_i y_j y_k$ ($-4 \leq i \leq j \leq k \leq 4$).

| Equation | Term | Coefficient | Equation | Term | Coefficient |
|----------|---------|---------------|----------|-------------|--------------|
| 3 | (0, 3) | $-3\sqrt{7}$ | 2 | (-2, 4) | $\sqrt{70}$ |
| | (-1, 4) | $\sqrt{42}$ | | (-1, 3) | $-\sqrt{14}$ |
| | (1, 2) | $3\sqrt{6}$ | | (0, 2) | $-\sqrt{3}$ |
| | (2, 1) | $-\sqrt{30}$ | | (1, 1) | $4\sqrt{2}$ |
| | (3, 0) | 3 | | (2, 0) | -7 |
| | | | (3, -1) | $\sqrt{30}$ | |
| 1 | (-3, 4) | $\sqrt{42}$ | 0 | (-3, 3) | $\sqrt{7}$ |
| | (-2, 3) | $\sqrt{14}$ | | (-2, 2) | $-\sqrt{3}$ |
| | (-1, 2) | $-2\sqrt{10}$ | | (-1, 1) | $-\sqrt{15}$ |
| | (0, 1) | $\sqrt{15}$ | | (0, 0) | 6 |
| | (1, 0) | 1 | | (1, -1) | $-\sqrt{15}$ |
| | (2, -1) | $-4\sqrt{2}$ | | (2, -2) | $-\sqrt{3}$ |
| | (3, -2) | $3\sqrt{6}$ | | (3, -3) | $\sqrt{7}$ |

Table A1. Coefficients for the quadratic "mixed" $\ell = 3$ map $Q^{(1)}$

| Equation | Term | Coefficient | Equation | Term | Coefficient |
|----------|-------|---------------|----------|-------|--------------|
| 4 | (13) | $-\sqrt{42}$ | 3 | (03) | $3\sqrt{7}$ |
| | (22) | $\sqrt{70}/2$ | | (12) | $\sqrt{14}$ |
| 2 | (02) | $-\sqrt{3}$ | 1 | (01) | $\sqrt{15}$ |
| | (11) | $\sqrt{10}$ | | (-12) | $-4\sqrt{2}$ |
| | (-13) | $-6\sqrt{3}$ | | (-23) | $-\sqrt{30}$ |
| 0 | (00) | 3 | | | |
| | (-11) | -1 | | | |
| | (-22) | -7 | | | |
| | (-33) | -3 | | | |

Table A2. Coefficients for the quadratic "mixed" $\ell = 4$ map $Q^{(2)}$

| Equation | Term | Coefficient | Equation | Term | Coefficient |
|----------|-------|----------------|----------|-------|---------------|
| 4 | (04) | 14 | 3 | (-14) | $7\sqrt{10}$ |
| | (13) | $-7\sqrt{10}$ | | (03) | -21 |
| | (22) | $3\sqrt{70}/2$ | | (12) | $\sqrt{70}$ |
| 2 | (-24) | $3\sqrt{70}$ | 1 | (-34) | $7\sqrt{10}$ |
| | (-13) | $-\sqrt{70}$ | | (-23) | $\sqrt{70}$ |
| | (02) | -11 | | (-12) | $-6\sqrt{10}$ |
| | (11) | $3\sqrt{10}$ | | (01) | 9 |
| 0 | (00) | 9 | | | |
| | (-11) | -9 | | | |
| | (-22) | -11 | | | |
| | (-33) | 21 | | | |
| | (-44) | 14 | | | |

Table A3. Coefficients for the quadratic "pure" $\ell = 4$ map $Q^{(3)}$

| Equation | Term | Coefficient | Equation | Term | Coefficient |
|----------|-----------|---------------|----------|--------|---------------|
| 3 | (-333) | -45 | 2 | (-323) | -45 |
| | (-223) | 45 | | (-213) | $10\sqrt{15}$ |
| | (-113) | -15 | | (-222) | 20 |
| | (-122) | $-5\sqrt{15}$ | | (-103) | $-15\sqrt{2}$ |
| | (003) | 0 | | (-112) | -35 |
| | (012) | $15\sqrt{2}$ | | (002) | 30 |
| | (111) | $-2\sqrt{15}$ | | (011) | $\sqrt{30}$ |
| 1 | (-313) | -15 | 0 | (-303) | 0 |
| | (-322) | $-5\sqrt{15}$ | | (-312) | $-15\sqrt{2}$ |
| | (-203) | $-15\sqrt{2}$ | | (-202) | 60 |
| | (-212) | 35 | | (-211) | $-5\sqrt{6}$ |
| | (-1 - 13) | $-6\sqrt{15}$ | | (-101) | -36 |
| | (-102) | $2\sqrt{30}$ | | (000) | 18 |
| | (-111) | -41 | | | |
| | (001) | 18 | | | |

Table A4. Coefficients for the cubic "pure" $\ell = 3$ map $C^{(1)}$

| Equation | Term | Coefficient | Equation | Term | Coefficient |
|----------|---------|--------------------|----------|------------------|-------------------|
| 4 | (-444) | 30/7 | 3 | (-434) | 30/7 |
| | (-334) | -30/7 | | (-324) | $-5\sqrt{7}/2$ |
| | (-224) | -5/7 | | (-333) | 5/56 |
| | (-233) | $5\sqrt{7}/4$ | | (-214) | 15/4 |
| | (-114) | 45/14 | | (-223) | 135/56 |
| | (-123) | -15/4 | | (-104) | $-\sqrt{10}/4$ |
| | (004) | -13/7 | | (-113) | -65/56 |
| | (013) | $\sqrt{10}/4$ | | (-122) | $-45\sqrt{7}/56$ |
| | (022) | $3\sqrt{5/14}$ | | (003) | -17/28 |
| | (112) | $-5\sqrt{7}/14$ | | (012) | $23/4\sqrt{5/14}$ |
| | | | (111) | $-15/28\sqrt{7}$ | |
| 2 | (-424) | -5/7 | 1 | (-414) | -45/14 |
| | (-433) | $5\sqrt{7}/4$ | | (-423) | 15/4 |
| | (-314) | -15/4 | | (-304) | $-\sqrt{10}/4$ |
| | (-323) | -135/56 | | (-313) | -65/56 |
| | (-204) | $3\sqrt{10/7}$ | | (-322) | $-45\sqrt{7}/56$ |
| | (-213) | $45\sqrt{7}/28$ | | (-2-14) | $5\sqrt{7}/7$ |
| | (-222) | 0 | | (-203) | $23/4\sqrt{5/14}$ |
| | (-1-14) | $-10\sqrt{7}/28$ | | (-212) | 15/8 |
| | (-103) | $-23/4\sqrt{5/14}$ | | (-1-13) | $-45\sqrt{7}/28$ |
| | (-112) | -15/8 | | (-102) | $3\sqrt{10}/4$ |
| | (002) | 7/2 | | (-111) | -25/8 |
| | (011) | $-3\sqrt{10}/8$ | | (001) | 1 |
| 0 | (-404) | -26/7 | | | |
| | (-413) | $\sqrt{10}/4$ | | | |
| | (-422) | $3\sqrt{70}/14$ | | | |
| | (-3-14) | $\sqrt{10}/4$ | | | |
| | (-303) | 17/14 | | | |
| | (-312) | $-23/4\sqrt{5/14}$ | | | |
| | (-2-24) | $3\sqrt{5/14}$ | | | |
| | (-2-13) | $-23/4\sqrt{5/14}$ | | | |
| | (-202) | 7 | | | |
| | (-211) | $3\sqrt{10}/8$ | | | |
| | (-1-12) | $3\sqrt{10}/8$ | | | |
| | (-101) | -2 | | | |
| | (000) | 1 | | | |

Table A5. Coefficients for the cubic "pure" $\ell = 4$ map $C^{(2)}$

References

- [1] Ashwin P, Chossat P 1998 Attractors for robust heteroclinic cycles with continua of connections, *J. of Nonlinear Science* **8** 103-130.
- [2] Chossat P 2001 The bifurcation of heteroclinic cycles in systems of hydrodynamical type, *Journal on Continuous, Discrete and Impulsive System* **8a** 4, 575-590.
- [3] Armbruster D, Chossat P 1991 Heteroclinic orbits in a spherically invariant system, *Physica D* **50** 155-176.
- [4] Beltrame P, Travnikov V, Gellert M and Egbers C 2006 GEOFLOW: simulation of convection in a spherical shell under central force field in terrestrial and microgravity environments, *Nonlinear Processes in Geophysics* **13** 413-423.
- [5] Chossat P, Guyard F 1996 Heteroclinic cycles in bifurcation problems with $O(3)$ symmetry *J. of Nonlinear Science* **6** 201-238.
- [6] Chossat P, Guyard F and Lauterbach R 1999 Generalized heteroclinic cycles in spherically invariant systems and their perturbations, *J. of Nonlinear Science* **9** 479-524.
- [7] Chossat P, Lauterbach R and Melbourne I 1990 Steady-State bifurcation with $O(3)$ -symmetry *Archive for Rat. Mech. Analysis* **113** 313-376.
- [8] Chossat P, Lauterbach R 2000 *Equivariant bifurcation theory and its applications* Advanced Series in Nonlinear Dynamics **15** World Scientific, Singapur.
- [9] Egbers C, Beyer W, Bonhage A, Hollerbach R and Beltrame P 2003 The geoflow-experiment on ISS (part I): Experimental preparation and design of laboratory testing hardware *Advances in Space Research* **32** 2, 171-180.
- [10] Field M 1989 Equivariant bifurcation theory and symmetry breaking *J. Dyn. Diff. Equat* **1** 369-421.
- [11] Friedrich R and Haken H 1986 Static, wavelike and chaotic thermal convection in spherical geometries *Phys. Rev. A* **34** 2100-2120.
- [12] Geiger C, Dangelmayr G, Rodriguez J D and Guttinger W 1993 Symmetry breaking bifurcations in spherical Benard convection. I: Results from singularity theory *Fields Institute Communications* **5** American Mathematical Society, Providence, RI, 225-237.
- [13] Gellert M, Beltrame P and Egbers C 2005 The GeoFlow experiment - spherical Rayleigh-Bénard convection under the influence of an artificial central force field *Journal of Physics: Conference Series* **14** 157-161.
- [14] Golubitsky M, Stewart I and Schaeffer D 1988 *Singularities and groups in bifurcation theory* Vol. 2, Appl. Math. Sci. **69** Springer Verlag.
- [15] Krupa M and Melbourne I 1995 Asymptotic stability of heteroclinic cycles in systems with symmetry *Erg. Th. Dyn. Sys* **15** 121-147
- [16] Rodriguez J D, Geiger C, Dangelmayr G and Guttinger W 1996 Symmetry breaking bifurcations in spherical Benard convection. II: Numerical results *Fields Institute Communications* **5** American Mathematical Society, Providence, RI, 239-253.

